Original Article

Clinicopathologic characteristics and diagnostic methods of *RET* rearrangement in Chinese non-small cell lung cancer patients

Junnan Feng[1,2#^], Yan Li[3#], Bing Wei[1,2#], Lei Guo[3], Weihua Li[3], Qingxin Xia[4], Chengzhi Zhao[1,2], Jiawen Zheng[1,2], Jiuzhou Zhao[1,2], Rui Sun[1,2], Yongjun Guo[1,2], Luka Brcic[5], Taiki Hakozaki[6], Jianming Ying[3], Jie Ma[1,2]

[1]Department of Molecular Pathology, Clinical Pathology Center, The Affiliated Cancer Hospital of Zhengzhou University, Henan Cancer Hospital, Zhengzhou, China; [2]Henan Key Laboratory of Molecular Pathology, Zhengzhou, China; [3]Department of Pathology, National Cancer Center/National Clinical Research Center for Cancer/Cancer Hospital, Chinese Academy of Medical Sciences and Peking Union Medical College, Beijing, China; [4]Department of Pathology, The Affiliated Cancer Hospital of Zhengzhou University, Henan Cancer Hospital, Zhengzhou, China; [5]Diagnostic and Research Institute of Pathology, Medical University of Graz, Graz, Austria; [6]Department of Thoracic Oncology and Respiratory Medicine, Tokyo Metropolitan Cancer and Infectious Diseases Center of Komagome Hospital, Tokyo, Japan

Contributions: (I) Conception and design: J Ma, J Ying; (II) Administrative support: None; (III) Provision of study materials or patients: L Guo, Q Xia; (IV) Collection and assembly of data: J Feng, Y Li; (V) Data analysis and interpretation: J Feng, Yan Li, B Wei; (VI) Manuscript writing: All authors; (VII) Final approval of manuscript: All authors.

[#]These authors contributed equally to this work.

Correspondence to: Jie Ma. Department of Molecular Pathology, Clinical Pathology Center, The Affiliated Cancer Hospital of Zhengzhou University, Henan Cancer Hospital, No. 127 Dongming Road, Jinshui District, Zhengzhou 450008, China. Email: zlyymajie0621@zzu.edu.cn; Dr. Jianming Ying. Department of Pathology, National Cancer Center/National Clinical Research Center for Cancer/Cancer Hospital, Chinese Academy of Medical Sciences and Peking Union Medical College, No. 17 Panjiayuan Nanli, Chaoyang District, Beijing 100021, China. Email: jmying@cicams.ac.cn.

Background: Rearranged during transfection (*RET*) rearrangement has been identified as one of the crucial oncogenic drivers in non-small cell lung cancer (NSCLC). Recently, two highly selective *RET* inhibitors have been approved by the US Food and Drug Administration and demonstrated remarkable responses. However, the clinical characteristics, outcomes and optimal diagnostic method of *RET*-rearrangements are not well understood. This study sought to evaluate the prevalence and characteristics of *RET* rearrangement, identify an effective diagnostic method for it, and correlate its presence with outcomes.

Methods: A total of 9,431 Chinese NSCLCs from two cancer centers who have undertaken targeted DNA-NGS were enrolled and 167 *RET*-positive cases were screened. Non-canonical *RET* rearrangements were confirmed by targeted RNA-NGS. If material was sufficient, positive cases were analyzed by fluorescence in situ hybridization (FISH) (n=30) and immunohistochemistry (IHC) (n=57). Clinicopathologic characteristics, molecular profiling and treatment outcomes of *RET* rearrangement were evaluated.

Results: The prevalence of *RET* rearrangement was 1.52% (138/9,101) in unfiltered cases and 8.79% (29/330) in *EGFR/KRAS/BRAF/ALK*-negative cases. *RET* rearrangement was common in females, never smokers, and lung adenocarcinoma patients. Additionally, 40.3% of stage IV *RET*-rearranged NSCLC patients developed brain metastases. *TP53* was the most common concurrent mutation, and 8 patients harbored concurrent driver oncogenic alterations, including *EGFR* (N=5), *KRAS* (N=2), and *ALK* (N=1). Non-canonical fusion partners were identified in 13.8% (23/167) of cases by DNA-based NGS, and RNA-based NGS identified 3 new partners (*EPS8*, *GOLGA5*, and *TNIP1*). The concordance of FISH and NGS was 83.3% (25/30), while the concordance of IHC and NGS was only 28.1% (16/57). Both IHC and FISH demonstrated lower sensitivity for *NCOA4*-/other-*RET* fusions. The *CCDC6-RET* subgroup had significantly

^ ORCID: 0000-0001-9588-4096.

longer progression-free survival than the *KIF5B-RET* subgroup, both after chemotherapy (23 *vs.* 9.7 months; P=0.014).

Conclusions: *RET* rearrangement occurs in 1.52% of Chinese NSCLCs and has identifiable clinicopathologic characteristics. *RET* IHC has a low sensitivity, disavowing its use in routine practice. While NGS and FISH has good performance in identifying *RET* rearrangement. Both IHC and FISH demonstrated lower sensitivity for *NCOA4-*/others-*RET* fusions. Clinical benefit with chemotherapy is different between *CCDC6-RET* and *KIF5B-RET* fusion patients, optimal treatment should be considered when selecting therapies for patients with *RET*-rearranged lung cancers.

Keywords: Rearranged during transfection (*RET*); gene rearrangement; non-small cell lung cancer (NSCLC); next-generation sequencing (NGS); Chinese patients.

Submitted Jan 13, 2022. Accepted for publication Apr 15, 2022.
doi: 10.21037/tlcr-22-202
View this article at: https://dx.doi.org/10.21037/tlcr-22-202

Introduction

The discovery of targetable oncogenic drivers has led to significant improvements in the treatment of non-small cell lung cancer (NSCLC). Among these, a number of fusion drivers, such as anaplastic lymphoma kinase (*ALK*), c-ros oncogene 1 (*ROS1*), and rearranged during transfection (*RET*), have been described as rare oncogenic events and recommended for routine testing at diagnosis (1).

The *RET* proto-oncogene was first identified in 1985 by Takahashi *et al.* (2). It encodes a transmembrane receptor tyrosine kinase that plays a key role in the differentiation of the kidneys and nervous system (3,4). The rearrangement of *RET* can lead to the constitutive activation of the *RET* tyrosine kinase domain and the recruitment of downstream signaling cascades, such as MAP kinase (MAPK), phosphatidylinositol-3-kinase (PI3K)/Akt, and Janus kinase-signal transducer and activator of transcription (JAK-STAT) pathways, which promote tumorigenesis (5).

Several multi-kinase inhibitors (MKIs), such as vandetanib and cabozantinib, have been used for targeted therapy to treat advanced *RET*-rearranged NSCLC patients. However, MKIs sometimes leads to significant "off-target" side effects, such as nausea, diarrhea, and hypertension (6,7). Recently, novel *RET* tyrosine kinase inhibitors (TKIs) with high selectivity, including selpercatinib (LOXO-292) and pralsetinib (BLU-667), have been approved by the Food and Drug Administration (FDA) for the treatment of advanced *RET*-rearranged lung and thyroid cancer (8-10). Therefore, it is important to rapidly and accurately identify *RET*-positive cases.

However, due to the low prevalence of *RET* fusions, there is only limited information about the clinical characteristics and outcomes of *RET*-rearranged NSCLC, especially in Chinese patients. Incidence of *RET* rearrangement ranges from 1% to 2% in NSCLC (11-13), and depends on the age, sex, smoking history and histological subtype. Different fusion partners have been identified in NSCLC, with the most major proportion being *KIF5B* (14). *RET* rearrangements tend to be mutually exclusive with other driver mutations in NSCLC such as *EGFR*, *KRAS*, *ALK* and *ROS1*, and associate with low PD-L1 expression (15) and low tumor mutation burden (16).

Furthermore, the screening methods for *RET* rearrangement have not yet been standardized. Several molecular diagnostic methods are used to identify gene fusions, including IHC, RT-PCR, FISH, and DNA/RNA-based NGS. Although IHC is an effective screening tool to detect *ALK*-positive patients, it showed low sensitivity (55–65%) and variable specificity (40–85%) in prior study (17) and may not be reliable to detect *RET* rearrangement. RT-PCR is specific, but it is limited to known fusion partners and thus may underestimate prevalence. *RET* FISH is highly sensitive (100%) but has suboptimal specificity (45–60%) (17,18). Moreover, break-apart displays low sensitivity in detecting non-canonical *RET* fusions (19). DNA-based NGS enables the detection of high-throughput genomic alterations and novel partners of gene rearrangement, but it fails to provide information on functional fusion transcripts (20). The main laboratory methods for *RET* rearrangements have not been systematically investigated and fully elucidated in NSCLC. Therefore, investigation of the prevalence, characteristics, and diagnostic methods

in a large cohort of NSCLC patients may provide comprehensive genomic profiling and optimal strategy for the selection of *RET*-rearranged patients.

This study analyzed the molecular profile of 9,431 Chinese NSCLC patients who underwent targeted DNA-based NGS in daily clinical practice at two large cancer centers and identified 167 *RET*-rearranged NSCLC cases. Different techniques, including RNA-based NGS, FISH, and IHC, were performed to investigate their performance. The prevalence, clinicopathologic characteristics, molecular profiling, and therapeutic outcomes of the *RET*-rearranged cases were analyzed. We present the following article in accordance with the REMARK reporting checklist (available at https://tlcr.amegroups.com/article/view/10.21037/tlcr-22-202/rc).

Methods

Patients and study design

This retrospective analysis included 9,431 NSCLC patients in a multi-center study from January 2017 to August 2020 (including the Henan Cancer Hospital, Zhengzhou, China and National Cancer Center/Cancer Hospital, Chinese Academy of Medical Science and Peking Union Medical College, Beijing, China). All patients who met the following criteria were included in the analysis: confirmed NSCLC by pathology; detected the mutations by NGS (8/56 cancer-related genes). Altogether, the cohort included 9,101 NSCLC patients without mutation-based pre-selection and 330 epidermal growth factor receptor (*EGFR*)/KRAS proto-oncogene (*KRAS*)/B-Raf proto-oncogene (*BRAF*)/*ALK*-negative patients (*EGFR/KRAS/BRAF* mutation status was tested by PCR, and *ALK* fusion status was tested by IHC-Ventana) (*Figure 1*). *RET*-positive cases were collected and analyzed. RNA-NGS were performed in non-canonical fusion subtypes. FISH (N=30) and IHC (N=57) assays were performed in *RET*-rearranged patients with sufficient tissue. Patients' medical records were retrospectively reviewed to collect data on age, sex, smoking status, tumor stage at diagnosis, pathological diagnosis, and treatment histories. The stage of each patient was assessed following American Joint Committee on Cancer Staging Manual version 7. The study was conducted in accordance with the Declaration of Helsinki (as revised in 2013). The study was approved by the local ethics committee of The Affiliated Cancer Hospital of Zhengzhou University (No. 2021-KY-0092), and was also approved by the institutional review board of National Cancer Center/Cancer Hospital, Chinese Academy of Medical Science and Peking Union Medical College (No. 20/444-2640). Written informed consent was obtained from all individuals included in the study.

Targeted DNA-NGS

Genomic DNA from formalin-fixed paraffin embedded (FFPE) tissue was isolated using the QIAamp DNA FFPE Tissue Kit (Qiagen, Duesseldorf, Germany). Libraries were prepared using commercial panels (Burning rock Technology, Guangzhou, China). Briefly, a panel covering 8 driver genes of NSCLC was used on 4,320 patients from the Henan Cancer Hospital. A panel covering 56 cancer-related genes was used on the other patients enrolled in the study, as previously reported (21). Samples were sequenced on the Nextseq 550 (Illumina, San Diego, CA, USA) with an average depth of 1,000×. All the reads were mapped to human genome 19, and alignments were visualized using the Integrative Genomics Viewer.

Targeted RNA-NGS

Total RNA from the FFPE tissue was extracted using the Magen FFPE DNA/RNA kit (Magen, Guangzhou, China). The quantity and quality of RNA were detected using the Qubit RNA HS Assay Kit (Thermo Fisher Scientific) and the RNA Pico Sensitivity Reagent Kit (PerkinElmer), respectively. Libraries were prepared using the commercial panel (Burning rock Technology) containing 115 fusions and splice-region variants, which covered the entire coding region of *RET*. NGS was performed on the Novaseq-6000 platform (Illumina) with at least 25M reads per sample.

FISH and IHC

FISH was performed using the *RET* (10q11) dual-color break-apart rearrangement probe (LBP Medicine Science and Technology, Guangzhou) and following the manufacturer's instructions. For each sample, >100 tumor cells were evaluated. Samples were considered *RET*-rearrangement when ≥15% of the tumor cells showed split signals or isolated 3' signals. Isolated 5' signals were thought to result from the deletion of the kinase domain and were considered negative. IHC was performed using a rabbit monoclonal anti-*RET* (EPR2871) antibody (ab134100, Abcam, Cambridge, MA). *RET* expression was evaluated according to the following intensity scores: 0: negative; 1+:

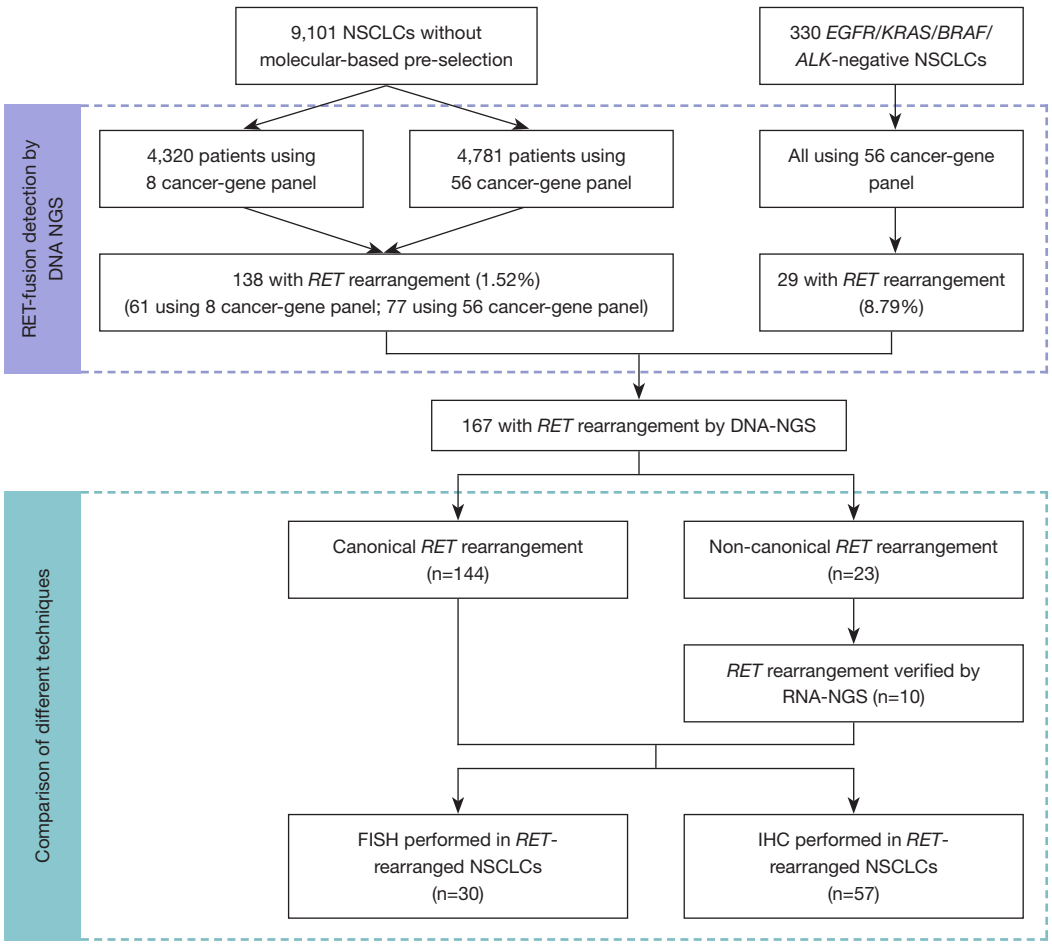

Figure 1 Study flow charts. A total of 9,431 patients from the Henan Cancer Hospital and the National Cancer Center/Cancer Hospital, Chinese Academy of Medical Science were enrolled in this study from January 2017 to August 2020. NSCLC, non-small cell lung cancer; *RET*, rearranged during transfection; NGS, next-generation sequencing; IHC, immunohistochemistry; FISH, fluorescence in situ hybridization.

weak; 2+: moderate, and 3+: strong in >10% of tumor cells. The FISH and IHC results were evaluated by 2 pathologists independently, blinded to the NGS results. We evaluated the *RET*-fusion using NGS as the reference standard in this study. FISH and IHC assays were performed in *RET*-rearranged patients with sufficient tissue. Consistency was defined as the percent of positive events to NGS results.

Statistical analysis

The Kaplan-Meier method was used to determine progression-free survival (PFS), and differences between groups were calculated using the log-rank test. The treatment response was assessed according to the Response Evaluation Criteria in Solid Tumors (RECIST) version 1.1 (22). All the statistical analyses were conducted using GraphPad Prism 5 software. The clinical characteristics of the different groups, including gender, age, smoking history, histology, and brain metastasis, were compared by the χ^2 test or Fisher exact test. Cox's proportional-hazards model was used to estimate the hazards ratio (HR) and the corresponding 95% confidence interval (95% CI) for the covariates of interests. Variables included sex, smoking, age, histology, stage, *RET*-rearranged subtype, breakpoint, distant metastasis, brain metastasis were selected for univariate analysis. Covariates with P value <0.10 from univariate analysis were considered for multivariable model. Statistical significance was defined as a 2-sided P value <0.05.

Table 1 Clinicopathological characteristics of *RET*-rearranged NSCLC patients (N=129)

Patient characteristics	No. (%) of patients (N=129)
Median age, years [range]	57 [30–83]
Gender	
Female	84 (65.1)
Male	45 (34.9)
Smoking	
Never	106 (82.2)
Smoker	23 (17.8)
Histology	
Adenocarcinoma	119 (92.3)
Squamous	2 (1.5)
Adenosquamous	5 (3.9)
Large cell carcinoma	1 (0.8)
Neuroendocrine carcinoma	2 (1.5)
Ki-67 (%)	
<20%	9 (7.0)
20–39%	13 (10.1)
40–59%	9 (7.0)
≥60%	18 (13.9)
NA	80 (62.0)
Stage at diagnosis	
I	37 (28.7)
II	7 (5.4)
III	23 (17.8)
IV	62 (48.1)
Distant metastasis (% of stage IV)	
No	16 (25.8)
Yes	46 (74.2)
Brain metastasis (% of stage IV)	
No	37 (59.7)
Yes	25 (40.3)

RET, rearranged during transfection; NSCLC, non-small cell lung cancer; NA, not available.

Results

Prevalence and characteristics of RET-rearranged NSCLC

In total, 167 *RET*-rearranged NSCLC patients were detected in our study. Among the 9,101 NSCLC patients without mutation-based pre-selection, 1.52% (138/9,101) were detected to have *RET* rearrangement, while in *EGFR/KRAS/BRAF/ALK*-negative NSCLC patients, the prevalence of *RET* rearrangement was 8.79% (29/330) (*Figure 1*).

The clinicopathological characteristics were accessible for 129 *RET*-rearranged NSCLC patients (*Table 1*). The median age at diagnosis was 57 years (range, 30–83 years). *RET* rearrangements were more frequent in females (65.1%) and never smokers (82.2%). The most common histological subtype of *RET*-rearranged NSCLC patients was lung adenocarcinoma (92.3%), but other subtypes were also detected, including squamous cell carcinoma (1.5%), large cell carcinoma (0.8%), and neuroendocrine carcinoma (1.5%). Among the 62 stage IV *RET*-rearranged patients, 74.2% (46/62) had distant metastasis, such as bone, brain, or liver metastasis. Notably, 40.3% (25/62) of the stage IV *RET*-rearranged patients had brain metastasis.

Partners of RET fusion

Among the 167 *RET* rearrangements, the most common fusion partner was *KIF5B* (68.2%, 114/167), followed by coiled-coil domain containing 6 (*CCDC6*) (16.8%, 28/167), and nuclear receptor coactivator 4 (*NCOA4*) (1.2%, 2/167) (*Figure 2A*). The breakpoint of *RET* was most frequently observed in intron 11, but other breakpoints included intron 10 and exon 11 (*Figure 2B*). In relation to the fusion partners, the most common breakpoints were *KIF5B* intron 15 (91% of *KIF5B-RET* patients) and *CCDC6* intron 1 (93% of *CCDC6-RET* patients) (*Figure 2C*).

Different characteristics were compared between the 90 *KIF5B-RET* patients and 23 *CCDC6-RET* patients with accessible clinical records (Table S1). The incidence of brain metastasis and distant metastasis in *KIF5B-RET* patients was higher than that in *CCDC6-RET* patients; however, the differences were not statistically significant.

Additionally, non-canonical fusion partners were also identified in 23 patients, including ADAM metallopeptidase

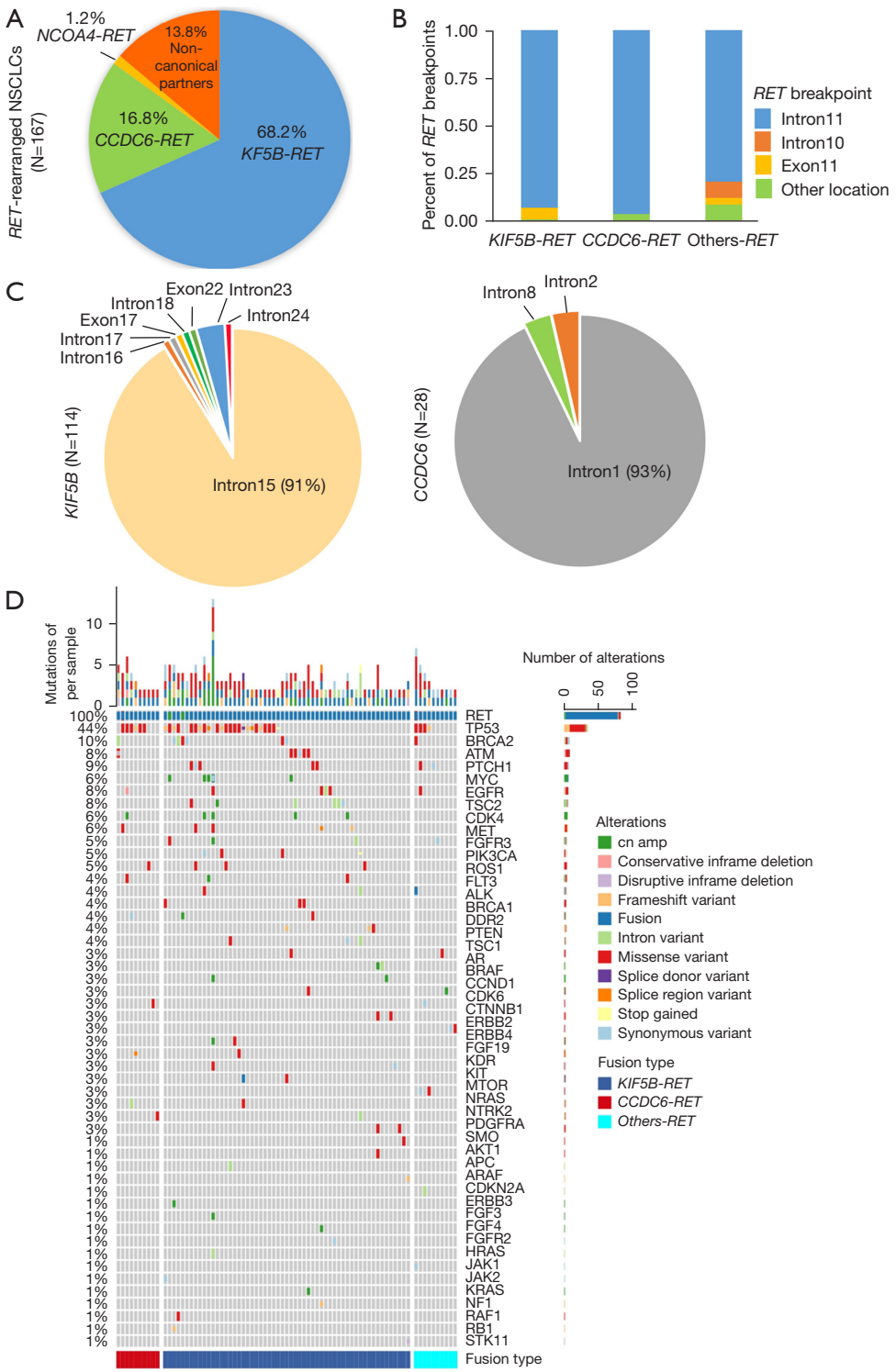

Figure 2 Overall landscape of *RET*-rearranged NSCLCs detected by NGS (N=167). (A) Proportions of different *RET* rearrangement partners; (B) percent of *RET* breakpoint positions according to the fusion subtypes; (C) distribution of *RET*-fusion partners' breakpoints; (D) concurrent genetic alteration analysis demonstrated by oncoPrint. The top bar indicates the number of mutations in each patient. The right-side bar demonstrates the number of patients harboring a specific mutation. Different colors indicate different mutation type categories. *RET*, rearranged during transfection; NSCLC, non-small cell lung cancer; NGS, next-generation sequencing.

with thrombospondin type 1 motif 2 (*ADAMTS2*), Rho GTPase activating protein 12 (*ARHGAP12*), centrosomal protein 128 (*CEP128*), epidermal growth factor receptor pathway substrate 8 (*EPS8*), and intergenic fusions. The relevant clinical information is listed in *Table 2*. Of the fusion partners, 3 have been reported as individual cases in the literature (23-25), but others have never been reported. RNA-based NGS was then performed to verify non-canonical *RET* rearrangement. Among the 23 non-canonical fusion cases, 10 cases had samples available for RNA-NGS and were all proven to have functional *RET* fusions at the RNA level (*Table 2*). It is of great clinical significance to evaluate the *RET*-TKI efficacy in such cases.

Mutation profile and concurrent driver gene alterations

As *Figure 1* shows, 106 *RET*-arranged patients were detected using 56 cancer-related gene panel. Co-occurring genetic aberrations were found in 77 patients (77/106, 73%). We constructed a heatmap to demonstrate the alterations co-occurring with the *RET* rearrangements (*Figure 2D*). Tumor protein 53 (*TP53*) was the most commonly altered (34/77, 44%), followed by *BRCA2* (8/77, 10%), *PTCH1* (7/77, 9%), *ATM* (6/77, 8%), *EGFR* (6/77, 8%), and *TSC2* (6/77, 8%). Other genomic alterations, including *MYC*, *CDK4*, *MET*, *FGFR3*, and *PIK3CA*, were also observed. Among the 106 *RET*-rearranged patients, 8 (7.55%) harbored concurrent driver gene alterations, including *EGFR* L858R (N=3), *EGFR* 19del (N=2), *KRAS* G12X (N=2), and *EML4-ALK* (N=1) (for further details, see Table S2).

Treatment and clinical outcomes of RET-rearranged NSCLC

Among the 129 *RET*-rearranged NSCLC patients with available treatment information, approximately 33.3% (43/129) underwent platinum-based doublet chemotherapy as the first-line treatment, 22.5% (29/129) received chemotherapy combined with antiangiogenic therapy as the first-line treatment, and 3.1% (4/129) received immune checkpoint inhibitors in clinical trials (*Figure 3A*). To evaluate the chemotherapy efficacy among different subtypes, the survival data of 36 late-stage patients were analyzed, including 28 *KIF5B-RET* patients and 8 *CCDC6-RET* patients. We found that patients with the *CCDC6-RET* subtype had significantly longer PFS than those with the *KIF5B-RET* subtype (23 *vs.* 9.7 months; P=0.014) (*Figure 3B*). Additionally, no significant difference was observed between the different breakpoints of *RET* (intron 11 *vs.* other locations) (*Figure 3B*). As *KIF5B-RET* patients appeared to suffer from brain and distant metastasis more than *CCDC6-RET* patients (Table S1; albeit the difference was not statistically significant), *RET*-rearranged subtypes were included in the Cox proportional-hazards model with other clinical characteristics. The results of the univariate and multivariate Cox proportional-hazards model based on the 36 *RET*-rearranged cases are listed in Table S3. Covariates with a P value <0.10 in the univariate analysis were included in the multivariable model. According to the multivariable analysis, *CCDC6-RET* cases had significantly better PFS than *KIF5B-RET* cases (HR =0.192, 95% CI: 0.044–0.831; P=0.027). Research with a sufficiently large cohort needs to verify these findings.

Only 4.7% (6/129) of the patients had access to *RET*-TKI, mainly due to the inaccessibility of *RET*-TKI at that time. A 54-year-old male with poorly differentiated lung adenocarcinoma had disease progression after receiving surgery, radiotherapy, and chemotherapy. The targeted NGS revealed an *ERC1-RET* fusion. Subsequently, after being started on Cabozantinib, SD was achieved. The patient continued to receive Cabozantinib treatment for 10 months before disease progression with new lung metastasis (Figure S1).

None of the 8 patients with concurrent driver gene alterations received *RET*-TKI treatment. One lung adenocarcinoma patient (Case No. 1) with *EGFR* L858R and *KIF5B-RET* has received Icotinib for almost 2 years and achieved stable disease (SD). When the patient's disease progressed, *KIF5B-RET* continued to be detected, but *EGFR* L858R disappeared. Another lung adenocarcinoma patient with *EGFR* 19del (Case No. 5) has been receiving Gefitinib for 2 years, and *CCDC6-RET* was detected as a resistant mechanism in the *EGFR*-TKI relapsed tumor (Table S2).

Detection of RET rearrangement

Among the 167 *RET*-positive cases detected by DNA-NGS, 144 were canonical fusion subtypes, and 23 were non-canonical fusion subtypes. A total of 10 non-canonical fusion samples were available for RNA-NGS, and all were proven to have functional *RET* fusions at the RNA level (*Table 2*). Representative fusion patterns at DNA and RNA levels are shown in Figure S2 using IGV.

FISH (N=30) and IHC (N=57) assays were performed in *RET*-rearranged patients with sufficient tissue. The FISH

Table 2 Non-canonical fusion cases and their relevant clinical information (N=23)

Fusion	Breakpoints	Locus of the partner gene	Gender	Age (years)	Histology	Literature	RNA-NGS results	FISH	IHC
ADAMTS2-RET	Intron10_Exon3	5q35.3	M	54	ADC	NA	NA	NA	NA
ARHGAP12-RET	Intron4_Intron11	10p11.22	F	65	ADC	NA	*KIF5B-RET* (Exon15_Exon12)	+	1+
CEP128-RET	Intron18_Intron10	14q31.1	F	63	ADC	NA	NA	NA	NA
EPS8-RET	Intron12_Intron11	12p12.3	F	56	ADC	NA	*EPS8-RET* (Exon12_Exon12)	NA	1+
ERC1-RET	Intron8_Intron11	12p13.33	M	54	ADC	PMID: 32737449	NA	NA	–
KIAA1217-RET	Intron1_Intron11	10p12.2-p12.1	F	70	ADC	PMID: 31162284	*KIF5B-RET* (Exon15_Exon12)	+	2+
PLCXD3-RET/ *LINC01264-RET*	Intron2_Intron11/ intergenic_Intron11	5p13.1; 10q11.21	M	83	ADC	NA	*KIF5B-RET* (Exon15_Exon12)	NA	NA
SLC6A11-RET	Intron5_Intron11	3p25.3	M	71	ADC	NA	NA	NA	NA
SPECC1L-DORA2A-RET	Intron10_Intron11	22q11.23	F	60	ADC	PMID: 31917708	NA	NA	NA
STK33-RET	Intron1_Intron11	11p15.4	F	65	ADC	NA	NA	NA	NA
BET1-RET	Intergenic_Intron11	7q21.3	F	56	ADC	NA	*KIF5B-RET* (Exon15_Exon12)	+	1+
CENPK-RET	Intergenic_Exon12	5q12.3	M	58	SCC	NA	NA	NA	NA
FXYD4-RET	Intergenic_Intron11	10q11.21	F	54	ADC	NA	NA	NA	NA
LINC00680-RET	Intergenic_Intron10	6p11.2	F	63	ADC	NA	*GOLGA5-RET* (Exon7_Exon12)	+	1+
KIAA0146-RET	Intergenic_Intron11	8q11.21	M	65	SCC	NA	NA	NA	NA
LOC105378330-RET	Intergenic_Intron11	10q21.3	F	64	ADC	NA	NA	NA	NA
LOC105378470-RET	Intergenic_Intron11	10q25.1	F	64	ADC	NA	*KIF5B-RET* (Exon15_Exon12)	NA	NA
LOC441666-RET	Intergenic_Intron11	10q11.21	F	67	ADC	NA	NA	NA	NA
MARCH8-RET	Intergenic_Intron11	10q11.21-q11.22	F	56	ADC	NA	*KIF5B-RET* (Exon15_Exon12)	+	2+
NAMPTL-RET	Intergenic_Intron11	10p11.21	F	49	AdCa	NA	NA	NA	NA
OR13A1-RET	Intergenic_Intron11	10q11.21	M	58	ADC	NA	NA	NA	NA
TNIP1-RET/ *RASGEF1A-RET*	Intron8_Intron11/ intergenic_Intron11	5q33.1; 10q11.21	M	65	ADC	NA	*TNIP1-RET* (Exon8_Exon12)	–	3+
TBC1D14-RET	Intergenic_Intron11	4p16.1	F	65	ADC	NA	*KIF5B-RET* (Exon15_Exon12)	NA	NA

F, female; M, male; ADC, adenocarcinoma; SCC, Squamous Cell Carcinoma; AdCa, Adenosquamous; NA, not available; FISH, fluorescence *in situ* hybridization; IHC, immunohistochemistry; –, negative; +, positive; 1+, weak; 2+, moderate; 3+, strong.

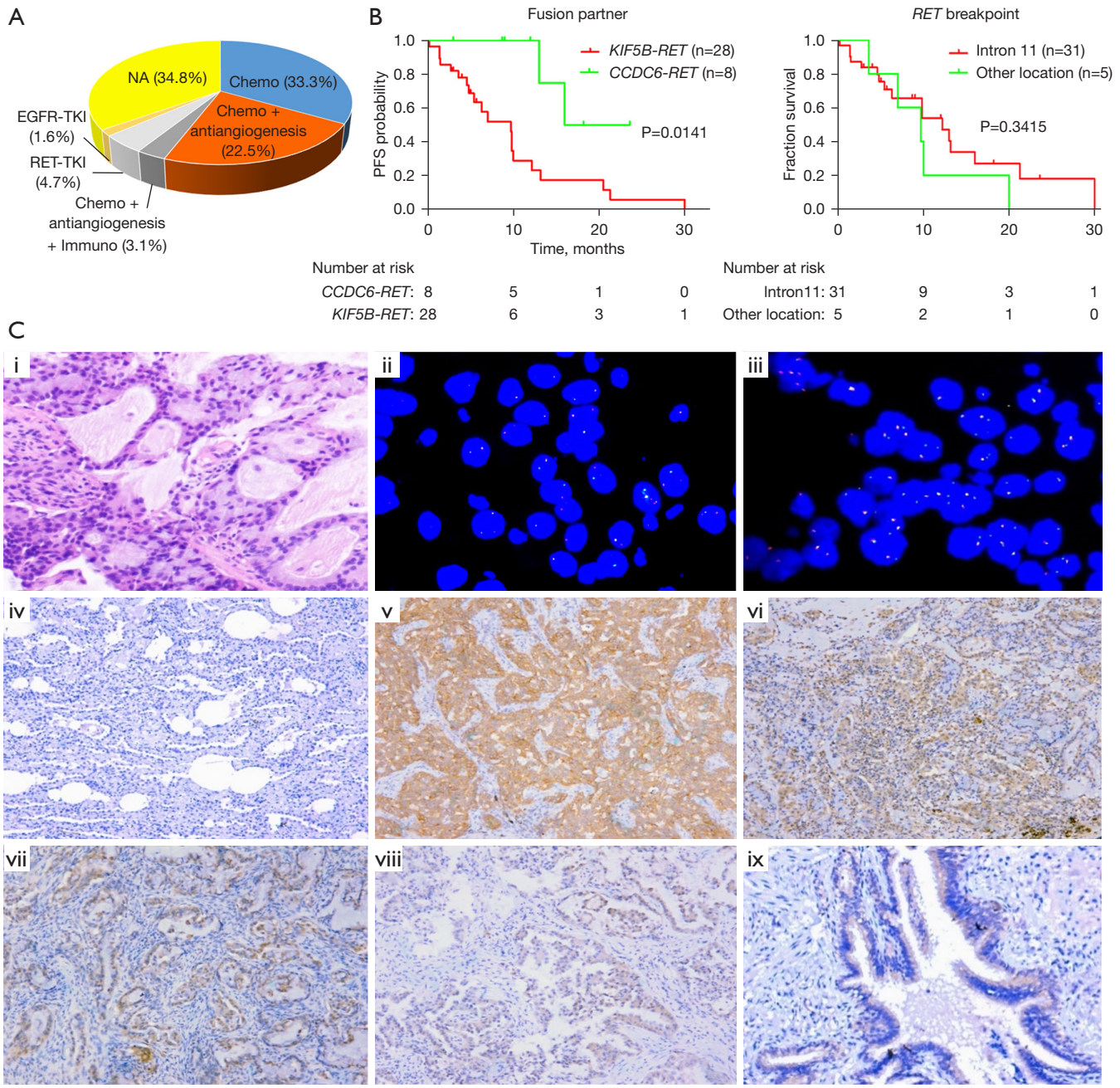

Figure 3 Outcomes of 129 *RET*-rearranged NSCLCs and representative FISH image and IHC staining pattern of *RET*-rearranged cases. (A) First-line treatment strategies of 129 *RET*-rearranged NSCLCs. (B) PFS analysis between *KIF5B-RET* and *CCDC6-RET* subtypes treated with chemotherapy (left). PFS analysis between different *RET* breakpoints in patients treated with chemotherapy (right). (C) *RET* FISH and IHC staining (i: 200×; ii-iii: 1,000×; iv-ix: 100×). HE-stained section of a lung adenocarcinoma with *RET* rearrangement (i). Representative image of *RET*-FISH using a break-apart probe (ii). Example of *RET* FISH testing showing equivocal signals (iii). *RET*-IHC negative NSCLC (iv). *RET*-IHC showing positive (3+) reaction in a *KIF5B-RET* case (v), 2+ positivity in a *KIF5B-RET* (vi), 2+ positivity in a *CCDC6-RET* case (vii), and a 1+ positivity in a *NCOA4-RET* case (viii). Expression of the *RET* protein was detected in nonneoplastic tracheal tissue (ix). *RET*, rearranged during transfection; NSCLC, non-small cell lung cancer; Chemo, platinum-based doublet chemotherapy; NA, not available; TKI, tyrosine kinase inhibitor; IHC, immunohistochemistry; HE, hematoxylin-eosin; FISH, fluorescence in situ hybridization; PFS, progression-free survival.

Table 3 Concordance of different *RET*-fusion testing techniques

Test result	NGS status				
	KIF5B-RET	*CCDC6-RET*	*NCOA4-RET*	Others-*RET*	All patients
RET-IHC					
N	39	12	2	4	57
3+	14	1	0	1	16
2+	14	5	0	0	19
1+	11	6	1	2	20
0	0	0	1	1	2
Concordance	35.9%	8.3%	0.0%	25.0%	28.1%
RET-FISH					
N	19	7	2	2	30
Positive	18	6	0	1	25
Negative	1	1	2	1	5
Concordance	94.7%	85.7%	0.0%	50.0%	83.3%

RET, rearranged during transfection; IHC, immunohistochemistry; FISH, fluorescence *in situ* hybridization; 0, negative; 1+, weak; 2+, moderate; 3+, strong; NGS, next-generation sequencing.

results revealed the *RET* rearrangement in 25/30 patients, resulting in the FISH/NGS concordance of 83.3% (*Table 3*). IHC intensity scores were 0 in 3.5% (2/57), 1+ in 35.1% (20/57), 2+ in 33.3% (19/57), and 3+ in 28.1% (16/57) of the *RET*-rearranged patients. IHC 3+ was considered positive, and the concordance of IHC and NGS was 28.1%. The staining pattern of *RET*-IHC varied in different fusion subtypes. Notably, *KIF5B-RET* showed diffuse, 2+/3+ cytoplasmic staining, while *CCDC6-RET* and others showed granular and patchy staining with weak intensity (*Figure 3C*). The normal tracheal epithelium also showed *RET*-IHC staining, which might lead to a staining pitfall in the interpretation of IHC results. We noted that IHC had extremely low sensitivity in non-*KIF5B-RET* patients (*CCDC6-RET*, 8%, *NCOA4-RET*, 0%, and other-*RET*, 25%), while FISH also showed unsatisfying sensitivity in non-*KIF5B-RET* patients. FISH or IHC were not able to detect *NCOA4-RET* cases.

Discussion

To the best of our knowledge, this study has one of the largest *RET*-rearranged NSCLC cohorts for which a comprehensive analysis of molecular profiling, clinical outcomes, and detection methods has been performed. This study enrolled 9,431 Chinese NSCLC patients, among whom NGS identified 167 *RET*-rearranged patients. In 9,101 Chinese NSCLC patients without molecular-based pre-selection, the prevalence of *RET* rearrangement was 1.52%, reflecting the findings of previous reports (26,27). In 330 *EGFR/KRAS/BRAF/ALK*-negative NSCLC patients, the prevalence of *RET* rearrangement was up to 8.8%, indicating the necessity of *RET* detection in NSCLC when other driver genes are negative. Similar to *ALK*- and *ROS1*-rearranged NSCLC (28), *RET* rearrangement was more common in female, never smokers, and lung adenocarcinoma patients. Importantly, 40.3% (25/62) of the stage IV *RET*-rearranged NSCLC patients had brain metastasis. This is much higher than the average brain metastasis rate reported for advanced NSCLC (10–20%) (29), and is especially high in *KIF5B-RET* patients (43%). Previous studies have also reported that *RET* fusion is an independent risk factor of brain metastasis (30,31). This observation may reinforce the importance of evaluating the intracranial therapeutic response of *RET*-TKIs based on the molecular subclass of tumors. Selective *RET* inhibitors, including pralsetinib and selpercatinib, have been approved by the FDA, and both of them have shown a significant ability to cross the blood-brain barrier (31-33).

To date, at least 15 *RET*-rearranged subtypes have been

reported in NSCLC, including *KIF5B-RET*, *CCDC6-RET* (34), *NCOA4-RET* (35), *TRIM33-RET* (36), *KIAA1217-RET* (37), *ERC1-RET* (38), and *MYO5C-RET* (39). In this study, diverse *RET* fusion partners were identified, including canonical partners, such as *KIF5B* (68.2%, 114/167), *CCDC6* (16.8%, 28/167), and *NCOA4* (1.2%, 2/167). Rare partners, such as *KIAA1217* and *TBC1D32*, were also identified, which have been reported in a previous study (40). Among the 23 non-canonical fusion subtypes identified in our study by DNA-NGS, 10 with sufficient tumor tissue were verified to harbor functional fusion transcripts by RNA-NGS, and 3 novel partners (*EPS8*, *GOLGA5*, and *TNIP1*) were found. Numerous breakpoints of *ALK* rearrangement have been reported to be associated with clinical benefits (17,41). However, the breakpoints of *RET* and its partners were relatively concentrated in our study, mainly in *RET* intron 11, *KIF5B* intron 15, and *CCDC6* intron 1 and no significant survival difference for chemotherapy was observed between the different *RET* breakpoints.

We also characterized the mutational profile of the *RET*-rearranged patients and found that *TP53* was the most common concurrent alteration. Previous studies have suggested that *TP53* concomitant mutations have a strong negative effect on the outcomes of patients with *EGFR*-mutant (42-45) and *ALK*-rearranged NSCLC (43,46,47). The poor prognostic effect of the *TP53* mutation on tumors may be due to the loss of tumor inhibitory function and the elevated level of genomic instability (48). It is generally believed that *RET* rearrangement occurs exclusively with other oncogenic drivers in treatment-naive lung cancers (49). However, 8 *RET*-rearranged NSCLC patients in our study harbored concurrent oncogenic driver gene alterations. *CCDC6-RET* was found to be a resistant mechanism in an *EGFR* L858R patient, and the 7 other *RET*-rearranged NSCLC patients with concurrent driver gene alterations were all treatment-naïve patients. Among these treatment-naïve patients, only one *KIF5B-RET* patient with *EGFR* L858R received *EGFR*-TKI Icotinib treatment, and that patient had a PFS time of 23 months. Intratumor heterogeneity may explain multi-driver gene alterations. Sun (50) and Kim (51) reported that *RET* fusion could occur as an acquired resistance mechanism to Osimertinib. Additionally, McCoach (52) reported that *RET* rearrangement could also act as an acquired resistance mechanism of *ALK*-TKI. Thus, we believe that screening for *RET* fusion in post-treatment settings is clinically significant.

Due to the inaccessibility of the *RET*-TKI at the time of diagnosis in our study cohort, most *RET*-rearranged patients received chemotherapy. Pemetrexed-based chemotherapy for NSCLC patients with *RET* fusion-positive metastatic NSCLC has been shown to provide a durable benefit (53). In our study, the *CCDC6-RET* subgroup had a significantly longer PFS than the *KIF5B-RET* subgroup. Tan *et al.* reported that overall survival was more prolonged in *CCDC6-RET* fusion than *KIF5B-RET* fusion-positive patients (54). However, the reasons for a better prognosis in *CCDC6-RET* than *KIF5B-RET* patients remain unclear.

Precision medicine for tumors depends on an effective and reliable detection method. This is even more important for mutations which exist only in a small proportion of patients. Ideally, molecular detection should be highly sensitive, specific, and feasible in most diagnostic laboratories. At present, there is no gold-standard for *RET* rearrangement detection. FISH has been the gold-standard assay for diagnosing *ALK*- and *ROS1*-fusions (55). It is available in most pathology laboratories, and has a low tumor tissue requirement. However, our study revealed that *RET* FISH might lead to false-negative results, especially in *CCDC6-RET* and non-canonical *RET*-fusion subtypes. Technically, the *RET* FISH test may be more challenging than most other break-apart assays, as *RET* and its most common fusion partners are situated very near to each other on chromosome 10 (approximately 7.9–17.9 Mb apart) and are thus difficult to interpret. Radonic indicated that FISH is a sensitive but unspecific technique for *RET* screening (56). *RET*-IHC has not generally been recommended in previous studies, as IHC is more likely to yield false-negative results (17,57,58), which was also observed in our study. The current impediments of *RET*-IHC include the low-level expression of the *RET*-fusion protein and the lack of specific antibodies. We also observed *RET* expression in the normal tracheal epithelium, which might lead to a false-positive result.

Targeted DNA-NGS in *RET* detection is accurate and comprehensive and thus provides a unique advantage in exploring novel partners and the simultaneous testing of multiple genes. However, DNA-NGS has limitations in identifying complex fusions, and RNA-NGS adds value to accurate detection (Figure S2). The discordance of *RET* fusion at the DNA and RNA level may be due to alternative splicing and the flexible break-induced repair mechanisms (59,60). Taking all these factors into consideration, we recommend DNA-NGS as a preliminary screening

strategy for patients who have been newly diagnosed. A FISH analysis may be an appropriate method when the specimens have too low tumor cell content. For unusual results of DNA-NGS or FISH, RNA-NGS can be used as a validation technique.

There are several limitations of our study. It is a retrospective study, in only two major centers. The NGS methods were not completely the same in the whole study cohort. Another limitation of our study is that due to the unavailability of targeting agents, the number of patients receiving *RET*-TKIs was small. Therefore, no correlation could be done between the clinical efficacy of *RET*-TKIs with fusion. We intend to conduct further studies that include more clinical features of *RET*-rearranged patients and prognostic evaluations of different *RET*-fusion subtypes.

Acknowledgments

The authors appreciate the academic support from the AME Lung Cancer Collaborative Group. The abstract has been presented at the Chinese Academic Conference on Tumor Biomarker (CCTB 2021).

Funding: This work was supported by the major public welfare projects in Henan Province (grant No. 201300310400) and the Technological and scientific projects in Henan Province (grant Nos. LHGJ20210175 and 222102310136).

Footnote

Reporting Checklist: The authors have completed the REMARK reporting checklist. Available at https://tlcr.amegroups.com/article/view/10.21037/tlcr-22-202/rc

Data Sharing Statement: Available at https://tlcr.amegroups.com/article/view/10.21037/tlcr-22-202/dss

Conflicts of Interest: All authors have completed the ICMJE uniform disclosure form (available at https://tlcr.amegroups.com/article/view/10.21037/tlcr-22-202/coif). LB reports that he has received grants from Takeda, Roche, BMS; payment or honoraria for lectures, presentations, speakers bureaus from Amgen, AstraZeneca, BMS, Eli Lilly, Janssen, MSD, Merck, Novartis; participation on an Advisory Boards of Eli Lilly, Janssen, MSD, Merck, Novartis. He is an International Secretary of the Austrian Society of Pathology, Member of Pulmonary Pathology Society Membership and Awards Committee, and Member of IASLC Mesothelioma Committee. TH has received payment for speakers bureaus from Chugai Pharmaceutical, outside the submitted work. The other authors have no conflicts of interest to declare.

Ethical Statement: The authors are accountable for all aspects of the work in ensuring that questions related to the accuracy or integrity of any part of the work are appropriately investigated and resolved. The study was conducted in accordance with the Declaration of Helsinki (as revised in 2013). The study was approved by the local ethics committee of The Affiliated Cancer Hospital of Zhengzhou University (No. 2021-KY-0092), and was also approved by the institutional review board of National Cancer Center/Cancer Hospital, Chinese Academy of Medical Science and Peking Union Medical College (No. 20/444-2640). Written informed consent was obtained from all individuals included in the study.

References

1. Lindeman NI, Cagle PT, Aisner DL, et al. Updated Molecular Testing Guideline for the Selection of Lung Cancer Patients for Treatment With Targeted Tyrosine Kinase Inhibitors: Guideline From the College of American Pathologists, the International Association for the Study of Lung Cancer, and the Association for Molecular Pathology. J Mol Diagn 2018;20:129-59.
2. Takahashi M, Ritz J, Cooper GM. Activation of a novel human transforming gene, ret, by DNA rearrangement. Cell 1985;42:581-8.
3. Ishizaka Y, Itoh F, Tahira T, et al. Human ret proto-oncogene mapped to chromosome 10q11.2. Oncogene 1989;4:1519-21.
4. Arighi E, Borrello MG, Sariola H. RET tyrosine kinase signaling in development and cancer. Cytokine Growth Factor Rev 2005;16:441-67.
5. Ibáñez CF. Structure and physiology of the RET

receptor tyrosine kinase. Cold Spring Harb Perspect Biol 2013;5:a009134.
6. Bronte G, Ulivi P, Verlicchi A, et al. Targeting RET-rearranged non-small-cell lung cancer: future prospects. Lung Cancer (Auckl) 2019;10:27-36.
7. Subbiah V, Cote GJ. Advances in Targeting RET-Dependent Cancers. Cancer Discov 2020;10:498-505.
8. Bradford D, Larkins E, Mushti SL, et al. FDA Approval Summary: Selpercatinib for the Treatment of Lung and Thyroid Cancers with RET Gene Mutations or Fusions. Clin Cancer Res 2021;27:2130-5.
9. Subbiah V, Shen T, Terzyan SS, et al. Structural basis of acquired resistance to selpercatinib and pralsetinib mediated by non-gatekeeper RET mutations. Ann Oncol 2021;32:261-8.
10. Markham A. Pralsetinib: First Approval. Drugs 2020;80:1865-70.
11. Li AY, McCusker MG, Russo A, et al. RET fusions in solid tumors. Cancer Treat Rev 2019;81:101911.
12. Takeuchi S, Yanagitani N, Seto T, et al. Phase 1/2 study of alectinib in RET-rearranged previously-treated non-small cell lung cancer (ALL-RET). Transl Lung Cancer Res 2021;10:314-25.
13. Zhang K, Chen H, Wang Y, et al. Clinical Characteristics and Molecular Patterns of RET-Rearranged Lung Cancer in Chinese Patients. Oncol Res 2019;27:575-82.
14. Stinchcombe TE. Current management of RET rearranged non-small cell lung cancer. Ther Adv Med Oncol 2020;12:1758835920928634.
15. Lu C, Dong XR, Zhao J, et al. Association of genetic and immuno-characteristics with clinical outcomes in patients with RET-rearranged non-small cell lung cancer: a retrospective multicenter study. J Hematol Oncol 2020;13:37.
16. Offin M, Guo R, Wu SL, et al. Immunophenotype and Response to Immunotherapy of RET-Rearranged Lung Cancers. JCO Precis Oncol 2019;3:PO.18.00386.
17. Ferrara R, Auger N, Auclin E, et al. Clinical and Translational Implications of RET Rearrangements in Non-Small Cell Lung Cancer. J Thorac Oncol 2018;13:27-45.
18. Baker JA, Sireci AN, Marella N, et al. Analytical Accuracy of RET Fusion Detection by Break-Apart Fluorescence In Situ Hybridization. Arch Pathol Lab Med 2022;146:351-9.
19. Yang SR, Aypar U, Rosen EY, et al. A Performance Comparison of Commonly Used Assays to Detect RET Fusions. Clin Cancer Res 2021;27:1316-28.
20. Xiang C, Guo L, Zhao R, et al. Identification and Validation of Noncanonical RET Fusions in Non-Small-Cell Lung Cancer through DNA and RNA Sequencing. J Mol Diagn 2022;24:374-85.
21. Li W, Zhang Z, Guo L, et al. Assessment of cytology based molecular analysis to guide targeted therapy in advanced non-small-cell lung cancer. Oncotarget 2016;7:8332-40.
22. Eisenhauer EA, Therasse P, Bogaerts J, et al. New response evaluation criteria in solid tumours: revised RECIST guideline (version 1.1). Eur J Cancer 2009;45:228-47.
23. Chu YH, Wirth LJ, Farahani AA, et al. Clinicopathologic features of kinase fusion-related thyroid carcinomas: an integrative analysis with molecular characterization. Mod Pathol 2020;33:2458-72.
24. Skálová A, Ptáková N, Santana T, et al. NCOA4-RET and TRIM27-RET Are Characteristic Gene Fusions in Salivary Intraductal Carcinoma, Including Invasive and Metastatic Tumors: Is "Intraductal" Correct?. Am J Surg Pathol 2019;43:1303-13.
25. Weisman PS, Altinok M, Carballo EV, et al. Uterine Cervical Sarcoma With a Novel RET-SPECC1L Fusion in an Adult: A Case Which Expands the Homology Between RET-rearranged and NTRK-rearranged Tumors. Am J Surg Pathol 2020;44:567-70.
26. Takeuchi K, Soda M, Togashi Y, et al. RET, ROS1 and ALK fusions in lung cancer. Nat Med 2012;18:378-81.
27. Lipson D, Capelletti M, Yelensky R, et al. Identification of new ALK and RET gene fusions from colorectal and lung cancer biopsies. Nat Med 2012;18:382-4.
28. Pan Y, Zhang Y, Li Y, et al. ALK, ROS1 and RET fusions in 1139 lung adenocarcinomas: a comprehensive study of common and fusion pattern-specific clinicopathologic, histologic and cytologic features. Lung Cancer 2014;84:121-6.
29. Saad AG, Yeap BY, Thunnissen FB, et al. Immunohistochemical markers associated with brain metastases in patients with nonsmall cell lung carcinoma. Cancer 2008;113:2129-38.
30. Wang H, Wang Z, Zhang G, et al. Driver genes as predictive indicators of brain metastasis in patients with advanced NSCLC: EGFR, ALK, and RET gene mutations. Cancer Med 2020;9:487-95.
31. Subbiah V, Velcheti V, Tuch BB, et al. Selective RET kinase inhibition for patients with RET-altered cancers. Ann Oncol 2018;29:1869-76.
32. Drilon A, Oxnard GR, Tan DSW, et al. Efficacy of Selpercatinib in RET Fusion-Positive Non-Small-Cell Lung Cancer. N Engl J Med 2020;383:813-24.
33. Gainor JF, Curigliano G, Kim DW, et al. Pralsetinib

for RET fusion-positive non-small-cell lung cancer (ARROW): a multi-cohort, open-label, phase 1/2 study. Lancet Oncol 2021;22:959-69.
34. Takeuchi K. Discovery Stories of RET Fusions in Lung Cancer: A Mini-Review. Front Physiol 2019;10:216.
35. Arai S, Kita K, Tanimoto A, et al. In vitro and in vivo anti-tumor activity of alectinib in tumor cells with NCOA4-RET. Oncotarget 2017;8:73766-73.
36. Wang M, Naganna N, Sintim HO. Identification of nicotinamide aminonaphthyridine compounds as potent RET kinase inhibitors and antitumor activities against RET rearranged lung adenocarcinoma. Bioorg Chem 2019;90:103052.
37. Lee MS, Kim RN, I H, et al. Identification of a novel partner gene, KIAA1217, fused to RET: Functional characterization and inhibitor sensitivity of two isoforms in lung adenocarcinoma. Oncotarget 2016;7:36101-14.
38. Drilon A, Rekhtman N, Arcila M, et al. Cabozantinib in patients with advanced RET-rearranged non-small-cell lung cancer: an open-label, single-centre, phase 2, single-arm trial. Lancet Oncol 2016;17:1653-60.
39. Lee SH, Lee JK, Ahn MJ, et al. Vandetanib in pretreated patients with advanced non-small cell lung cancer-harboring RET rearrangement: a phase II clinical trial. Ann Oncol 2017;28:292-7.
40. Subbiah V, Yang D, Velcheti V, et al. State-of-the-Art Strategies for Targeting -Dependent Cancers. J Clin Oncol 2020;38:1209-21.
41. Lin JJ, Zhu VW, Yoda S, et al. Impact of EML4-ALK Variant on Resistance Mechanisms and Clinical Outcomes in ALK-Positive Lung Cancer. J Clin Oncol 2018;36:1199-206.
42. Canale M, Petracci E, Delmonte A, et al. Impact of TP53 Mutations on Outcome in EGFR-Mutated Patients Treated with First-Line Tyrosine Kinase Inhibitors. Clin Cancer Res 2017;23:2195-202.
43. Canale M, Petracci E, Delmonte A, et al. Concomitant TP53 Mutation Confers Worse Prognosis in EGFR-Mutated Non-Small Cell Lung Cancer Patients Treated with TKIs. J Clin Med 2020;9:1047.
44. Labbé C, Cabanero M, Korpanty GJ, et al. Prognostic and predictive effects of TP53 co-mutation in patients with EGFR-mutated non-small cell lung cancer (NSCLC). Lung Cancer 2017;111:23-9.
45. Liu S, Yu J, Zhang H, et al. TP53 Co-Mutations in Advanced EGFR-Mutated Non-Small Cell Lung Cancer: Prognosis and Therapeutic Strategy for Cancer Therapy. Front Oncol 2022;12:860563.
46. Wang WX, Xu CW, Chen YP, et al. TP53 mutations predict for poor survival in ALK rearrangement lung adenocarcinoma patients treated with crizotinib. J Thorac Dis 2018;10:2991-8.
47. Costa DB. TP53 mutations are predictive and prognostic when co-occurring with ALK rearrangements in lung cancer. Ann Oncol 2018;29:2028-30.
48. Brosh R, Rotter V. When mutants gain new powers: news from the mutant p53 field. Nat Rev Cancer 2009;9:701-13.
49. Cancer Genome Atlas Research Network. Comprehensive molecular profiling of lung adenocarcinoma. Nature 2014;511:543-50.
50. Sun Y, Pei L, Luo N, et al. A Novel MYH9-RET Fusion Occurrence and EGFR T790M Loss as an Acquired Resistance Mechanism to Osimertinib in a Patient with Lung Adenocarcinoma: A Case Report. Onco Targets Ther 2020;13:11177-81.
51. Kim M, Na JM, Lee GW, et al. EGFR-mutated pulmonary adenocarcinoma with concurrent PIK3CA mutation, and with acquired RET fusion and EGFR T790M mutation after afatinib therapy. J Pathol Transl Med 2021;55:79-82.
52. McCoach CE, Le AT, Gowan K, et al. Resistance Mechanisms to Targeted Therapies in ROS1+ and ALK+ Non-small Cell Lung Cancer. Clin Cancer Res 2018;24:3334-47.
53. Drilon A, Bergagnini I, Delasos L, et al. Clinical outcomes with pemetrexed-based systemic therapies in RET-rearranged lung cancers. Ann Oncol 2016;27:1286-91.
54. Tan AC, Seet AOL, Lai GGY, et al. Molecular Characterization and Clinical Outcomes in RET-Rearranged NSCLC. J Thorac Oncol 2020;15:1928-34.
55. Shaw AT, Felip E, Bauer TM, et al. Lorlatinib in non-small-cell lung cancer with ALK or ROS1 rearrangement: an international, multicentre, open-label, single-arm first-in-man phase 1 trial. Lancet Oncol 2017;18:1590-9.
56. Radonic T, Geurts-Giele WRR, Samsom KG, et al. RET Fluorescence In Situ Hybridization Analysis Is a Sensitive but Highly Unspecific Screening Method for RET Fusions in Lung Cancer. J Thorac Oncol 2021;16:798-806.
57. Tsuta K, Kohno T, Yoshida A, et al. RET-rearranged non-small-cell lung carcinoma: a clinicopathological and molecular analysis. Br J Cancer 2014;110:1571-8.
58. Belli C, Penault-Llorca F, Ladanyi M, et al. ESMO recommendations on the standard methods to detect RET fusions and mutations in daily practice and clinical research. Ann Oncol 2021;32:337-50.

59. Mizukami T, Shiraishi K, Shimada Y, et al. Molecular mechanisms underlying oncogenic RET fusion in lung adenocarcinoma. J Thorac Oncol 2014;9:622-30.
60. Li W, Guo L, Liu Y, et al. Potential Unreliability of Uncommon ALK, ROS1, and RET Genomic Breakpoints in Predicting the Efficacy of Targeted Therapy in NSCLC. J Thorac Oncol 2021;16:404-18.

(English Language Editor: L. Huleatt)

Cite this article as: Feng J, Li Y, Wei B, Guo L, Li W, Xia Q, Zhao C, Zheng J, Zhao J, Sun R, Guo Y, Brcic L, Hakozaki T, Ying J, Ma J. Clinicopathologic characteristics and diagnostic methods of *RET* rearrangement in Chinese non-small cell lung cancer patients. Transl Lung Cancer Res 2022;11(4):617-631. doi: 10.21037/tlcr-22-202

Supplementary

Table S1 Clinicopathologic characteristics between *KIF5B-RET* cases (N=90) and *CCDC6-RET* cases (N=23)

Variables	*KIF5B-RET*, N=90 [%]	*CCDC6-RET*, N=23 [%]	χ^2	P
Gender			0.054	0.815
Female	61 [68]	15 [65]		
Male	29 [32]	8 [35]		
Smoking			0.425	0.514
Never	79 [88]	19 [83]		
Smoker	11 [12]	4 [17]		
Age (years)			0.175	0.674
≤60	59 [66]	14 [61]		
>60	31 [34]	9 [39]		
Histology			1.907	0.167
ADC	83 [92]	23 [100]		
Non-ADC	7 [8]	0 [0]		
Stage			1.306	0.727
I	28 [31]	6 [26]		
II	4 [4]	2 [9]		
III	14 [16]	5 [22]		
IV	44 [49]	10 [43]		
Distant metastasis (% of stage IV)			2.244	0.134
No	8 [18]	4 [40]		
Yes	36 [82]	6 [60]		
Brain metastasis (% of stage IV)			1.843	0.174
No	25 [57]	8 [80]		
Yes	19 [43]	2 [20]		

RET, rearranged during transfection; ADC, adenocarcinoma.

https://dx.doi.org/10.21037/tlcr-22-202

Table S2 Concurrent driver gene alteration in *RET*-rearranged NSCLCs

Case No.	Fusion	Concurrent mutations	Gender	Age	Histology	Stage	Treated with other TKI (PFS)
1	*KIF5B-RET* (K15:R12)	*EGFR* p.L858R	Male	41	ADC	III	Icotinib (PFS 23m)
2	*CEP128-RET* (C18:R11)	*EGFR* p.L858R	Female	63	ADC	IV	No
3	*LOC105378330-RET* (Lintergenic:R12)	*EGFR* p.L858R	Male	65	ADC	III	No
4	*NAMPTL-RET* (Nintergenic:R12)	*EGFR* p.19del	Female	49	ADC	III	No
5	*CCDC6-RET* (C1:R12)	*EGFR* p.19del	Female	50	ADC	IV	Gefitinib (PFS 24 m)*
6	*CCDC6-RET* (C1:R12)	*KRAS* p.G12V	Female	50	ADC	III	No
7	*SLC6A11-RET* (S5:R12)	*KRAS* p.G13D	Male	71	ADC	III	No
8	*ADAMTS2-RET* (A10:R3)	*EML4-ALK* (E6:A20)	Male	54	ADC	II	No

*, *CCDC6-RET* was detected as a resistant mechanism to *EGFR*-TKI in Case No 5. *RET*, rearranged during transfection; NSCLC, non-small cell lung cancer; ADC, adenocarcinoma; PFS, progression-free survival.

Table S3 Predictive factors for PFS in late-stage *RET*-rearranged NSCLCs with chemotherapy (N=36)

Variables	Univariable analysis, P	Multivariable analysis	
		Hazard ratio (95% CI)	P
Sex (female *vs.* male)	0.354	–	–
Smoking (never *vs.* ever)	0.828	–	–
Age(years) (≤60 *vs.* >60)	0.173	–	–
Histology (others *vs.* ADC)	0.386	–	–
Stage (III *vs.* IV)	0.429	–	–
Partner (*CCDC6 vs. KIF5B*)	0.014	0.192 (0.044–0.831)	0.027
Breakpoint (non-intron11 *vs.* intron11)	0.356	–	–
Distant Metastasis (no *vs.* yes)	0.083	–	0.724
Brain Metastasis (no *vs.* yes)	0.543	–	

NSCLC, non-small cell lung cancer; *RET*, rearranged during transfection; CI, confidence interval; ADC, adenocarcinoma.

https://dx.doi.org/10.21037/tlcr-22-202

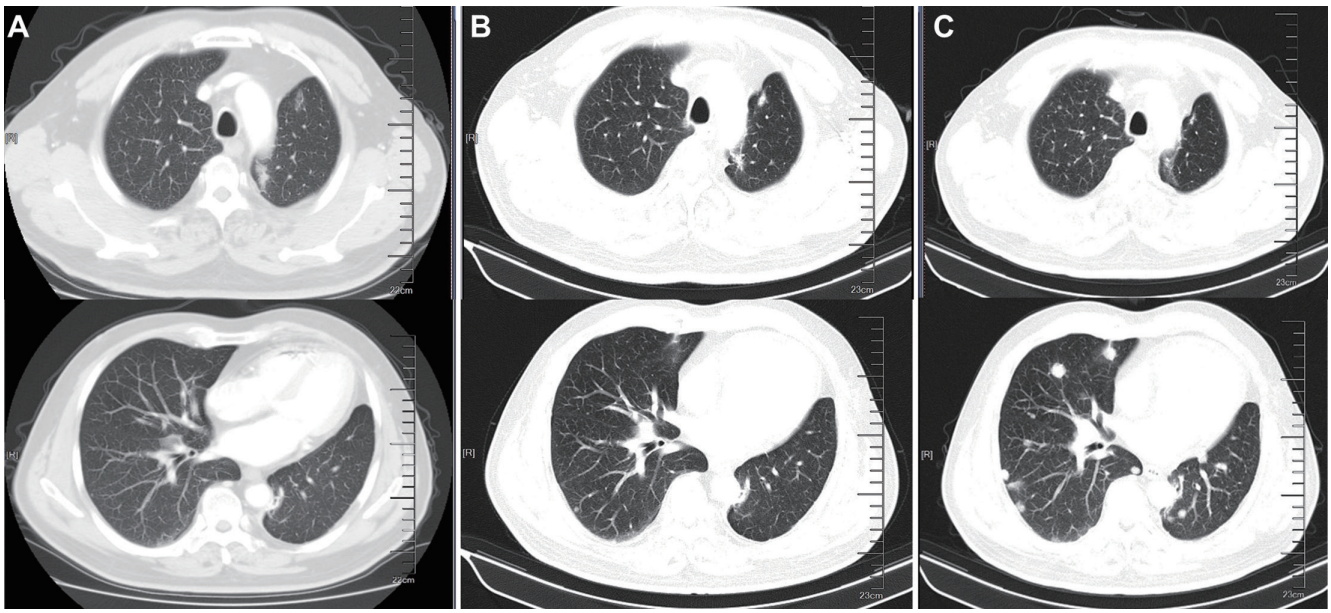

Figure S1 CT scans before and after therapy in a case of *ERC1-RET* fusion. (A) CT scans before Cabozantinib. (B) CT scans after 4 months of treatment with Cabozantinib. (C) CT scans after 10 months of treatment with Cabozantinib. CT, computed tomography.

https://dx.doi.org/10.21037/tlcr-22-202

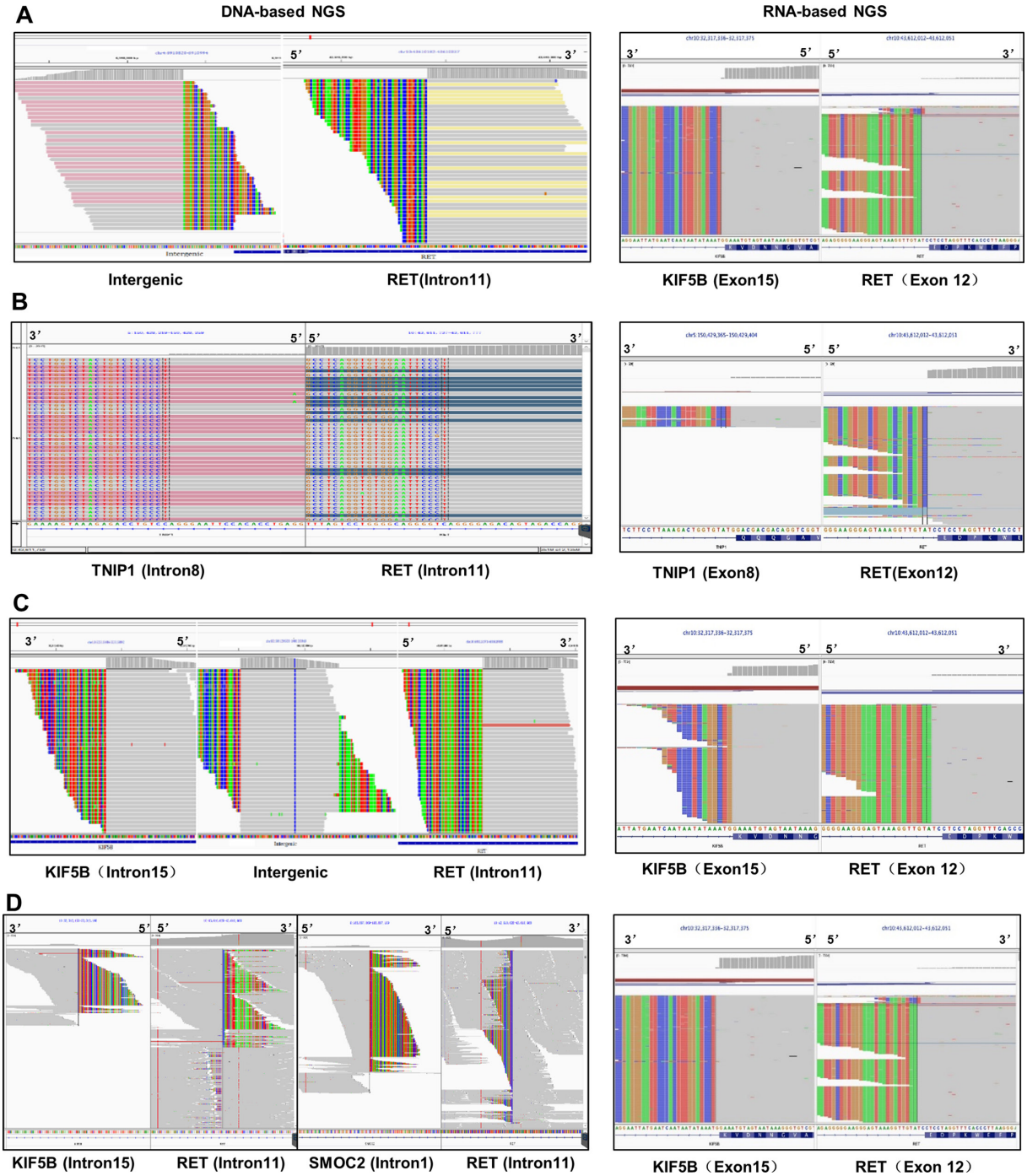

Figure S2 *RET* fusion identified by targeted DNA-NGS and RNA-NGS among 4 representative NSCLC cases. (A) DNA-based NGS revealed that the 3' portion of *RET* was fused to an intergenic region downstream of *TBC1D14*, while targeted RNA-NGS identified the *KIF5B-RET* (K15:R12) fusion transcript. (B) DNA-based NGS revealed *TNIP1-RET* (intron 8: intron 11), while targeted RNA-NGS identified the *TNIP1-RET* fusion transcript. (C) Targeted DNA-NGS revealed that the 3' portion of *RET* was fused to an intergenic region downstream of *LOC105378470* and then connected to the *KIF5B* gene after about 70 bp intervals, while targeted RNA-NGS identified the *KIF5B-RET* (K15:R12) fusion transcript. (D) *RET-KIF5B* (intron 11: intron 15) and *SMOC2-RET* (intron 1: intron 11) were detected simultaneously by targeted DNA-NGS, while canonical *KIF5B-RET* (K15:R12) fusion transcript was identified at the RNA level.

https://dx.doi.org/10.21037/tlcr-22-202